Supplemental Material

Journal of Climate

Modes of Variability in E3SM and CESM Large Ensembles

https://doi.org/10.1175/JCLI-D-23-0454.1

Supplementary Information for Modes of Variability in E3SM and CESM Large Ensembles

John T. Fasullo[1], Julie M. Caron[1], Adam Phillips[1], Hui Li[1], Jadwiga H. Richter[1], Richard B. Neale[1], Nan Rosenbloom[1], Gary Strand[1], Sasha Glanville[1], Yuanpu Li[1], Flavio Lehner[1], Gerald Meehl[1], Jean-Christophe Golaz[2], Paul Ullrich[2], Jiwoo Lee[2], Julie Arblaster[3]

1. *National Center for Atmospheric Research, Boulder, CO*
2. *Lawrence Livermore National Laboratory, Livermore, CA*
3. *School of Earth Atmosphere and Environment, Monash, University, AUS*

Corresponding author: Dr. John Fasullo, fasullo@ucar.edu

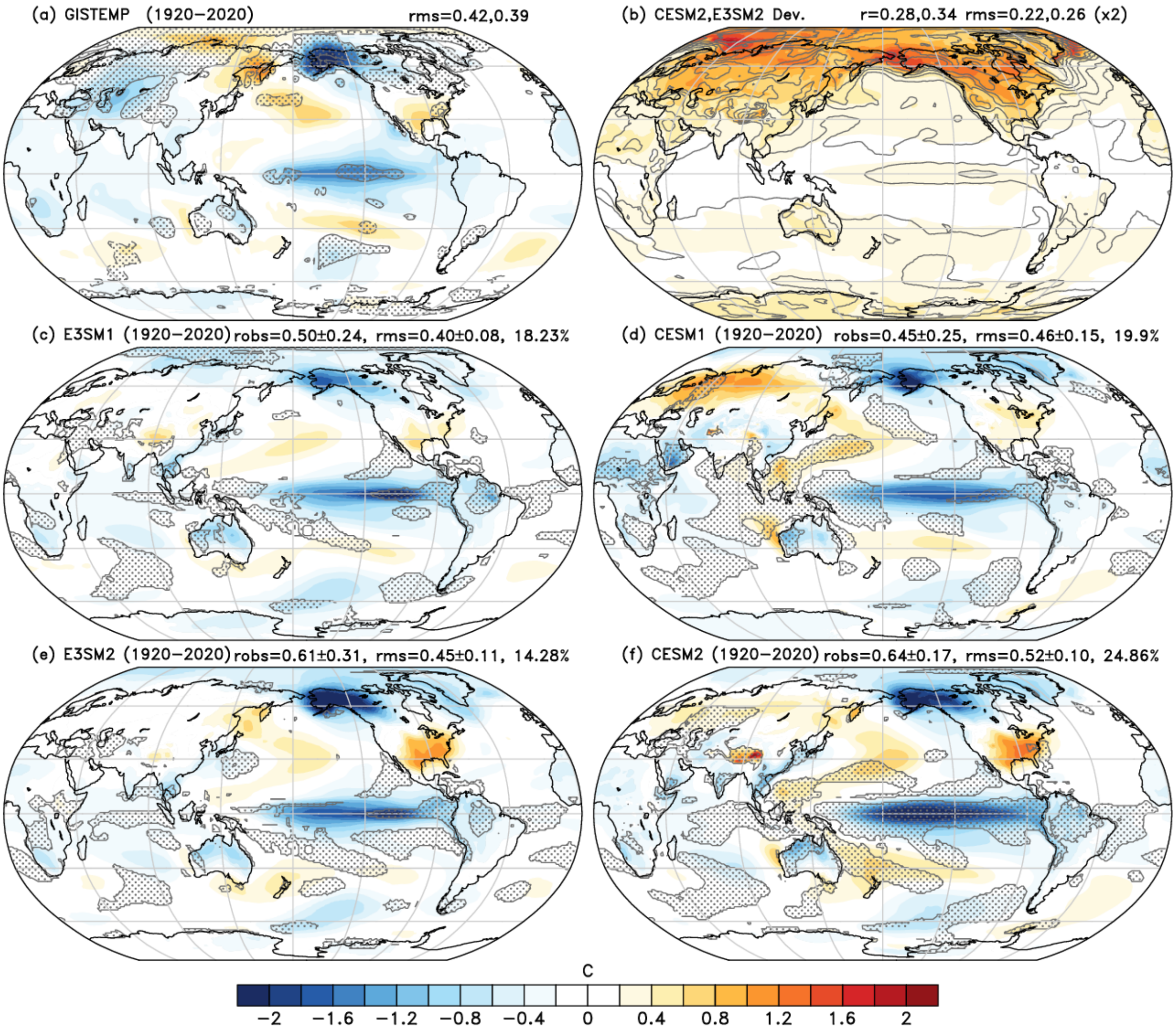

Fig. S1. The observed La Niña teleconnection pattern in T_{2m} (K) in DJF estimated from observations (GISTEMP, **a**) and the standard deviation in patterns across ensemble members from CESM2 (contours) and E3SM2 (lines, **b**). The ensemble-mean patterns estimated from E3SM1 (**c**), CESM1 (**d**), E3SM2 (**e**), and CESM2 (**f**) are also shown. Stippling in (**a**) where differences with GISTEMP exceed 0.2K and in (**c-f**) where observations lie outside of each ensemble. Values in the headers include (a) the RMS magnitude of the patterns in GISTEMP and BEST, (b) the pattern correlations with the respective simulated patterns and the RMS magnitudes, (c-f) the pattern correlation of ensemble members with the GISTEMP pattern and the 2 σ range, the mean RMS magnitude and 2 σ range, and the percentage of global area in which the observations lie outside of the 2 σ range.

The La Niña composite patterns, generated in an analogous fashion to the El Niño composite but for cool anomalies exceeding the standard deviation threshold, are shown in Figure S1 for DJF T_{2m} anomalies estimated from composites of events in nature using HadISST (Fig. S1a), the intra-ensemble standard deviation in the analogous patterns for

CESM2 (filled contours) and E3SM2 (contour lines, Fig. S1b), and the ensemble mean patterns from versions 1 and 2 of both E3SM and CESM (Fig. S1c-f). In observations the pattern is characterized by a zonally broad band of cool anomalies centered near 200 ^{o} E that extends further westward than warm anomalies during El Niño and about 5^{o} from the equator. Cool anomalies also exist in northern NA, and many subtropical land regions. As for El Niño teleconnections, intra-ensemble variability is particularly large over boreal land regions. In E3SM1, the anomalies are similar to those observed however they extend slightly too far west and are also too strong in the eastern EPO. Remote anomalies, and particularly those in NA are similar in strength and structure to those observed. Composite anomalies in all LEs share aspects of the E3SM1 biases, including the excessive westward extension of anomalies in the EPO. Teleconnections in E3SM2 and CESM2 strengthen relative to E3SM1 and CESM1 however teleconnections in most regions fall within the ensemble range. Pattern correlations with observations increase between both E3SM1 (r=0.50) and E3SM2 (r=0.61), and CESM1 (r=0.45) and CESM2 (r=0.64).

Figure S2 shows La Niña composite patterns with precipitation (P) estimated from composites of events in nature using GPCP (Fig. S2a), the intra-ensemble standard deviation in the analogous patterns for CESM2 (filled contours) and E3SM2 (contour lines, Fig. S2b), and the ensemble mean patterns from versions 1 and 2 of both E3SM and CESM (Fig. S2c-f). Observed precipitation teleconnections are characterized by a zonally broad band of strongly negative precipitation anomalies in the central and eastern EPO centered just west of the dateline that extends about 5^{o} from the equator and into the southern subtropics near 220^{o}E. It is surrounded to the north, west, and south by positive anomalies that extend into the midlatitudes. Negative precipitation anomalies exist off the west coast of NA, and over southeastern SA, and southern NA, where warm anomalies are associated with reduced precipitation (Fig. 4a). Positive precipitation anomalies span South Africa, much of Australia, and northern SA and thus these regions are also relatively cool during La Niña (Fig. S1a). Intra-ensemble variability in precipitation is distributed more evenly about the equator than during El Niño and is large over southern Africa, Australia, and SA. In all LEs, the anomalies are too narrowly confined to the EPO and extend too far to the west. Simulated pattern correlations increase between versions 1 and 2 of both E3SM (r=0.68 to r=0.73) and CESM (r=0.54 to r=0.68), as does the strength of simulated patterns. As for El Niño, the pattern strength in CESM2 is excessive.

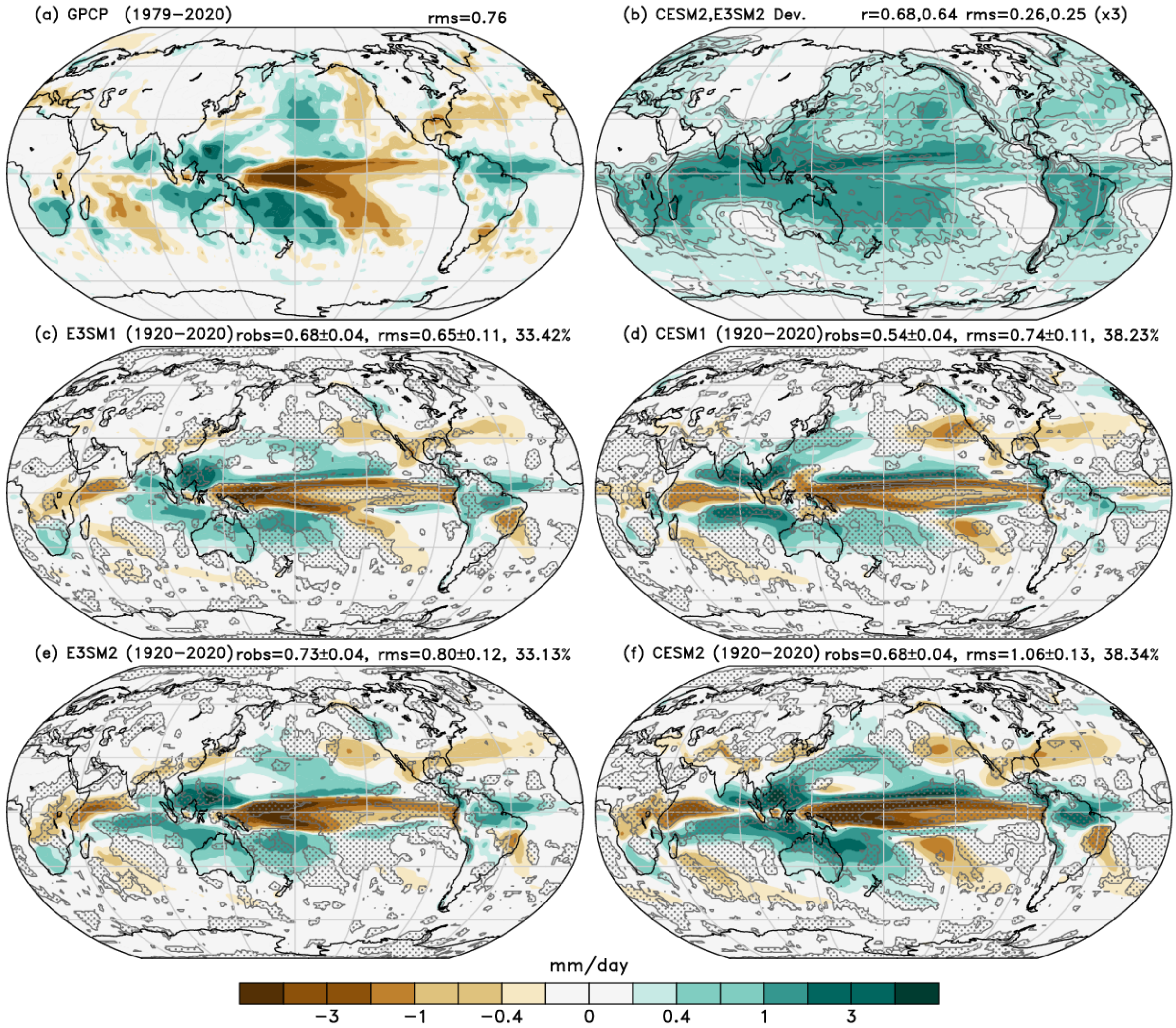

Fig. S2. The observed La Niña teleconnection pattern in PR (mm day^{-1}) in DJF estimated from observations (GPCP, **a**) and the standard deviation in the pattern across ensemble members from CESM2 (contours) and E3SM2 (lines, **b**). The ensemble-mean patterns estimated from E3SM1 (**c**), CESM1 (**d**), E3SM2 (**e**), and CESM2 (**f**) are also shown. Contours in (**c-f**) where observations lie outside of each ensemble. Metrics in the panel headers are consistent with those in Fig. 3.

Figure S3 shows La Niña's time-space structure in T_{2m} anomalies estimated from composites of events in nature using HadISST (Fig. S3a), the intra-ensemble standard deviation in the analogous structures for CESM2 (filled contours) and E3SM2 (contour lines, Fig. S3b), and the ensemble mean patterns from versions 1 and 2 of both E3SM and CESM (Fig. S3c-f). In observations, the pattern is characterized by cooling that extends from east of the dateline (~45ºE) to 110ºW that emerges in boreal summer, peaks from December to January (depending on longitude) and recedes in March through May. Unlike El Niño, La

Niña exhibits an evolution that suggests a westward propagation of anomalies. While La Niña events often transition from El Niño events, their multi-year character can also limit the expression of El Niño in the surrounding years of composite events, as evident by neutral anomalies in the January prior to La Niña and cool conditions in the following January (Fig. 8a). As a result, significant inter-member spread is also evident at the onset and termination of events (Fig. S3b). While the general character of composite anomalies in the LEs is similar to that observed, including their westward propagation, significant biases exist in both the magnitude and temporal evolution of events. Events in E3SM1 and E3SM2 are generally too biennial, as evident by the strong warm anomalies in the DJF periods prior to and following events in the composites. As for El Niño, a strong zonal gradient in variability is also evident in E3SM1 and E3SM2 that contrasts with the observed structure. A similar but weaker bias exists in CESM1 and CESM2 with event magnitude that is excessive, particularly in CESM2. Thus, while the pattern correlation of the composite improves between versions 1 and 2 of both E3SM (r=0.84 to r=0.85) and CESM (r=0.88 to r=0.89), the strength of the patterns shown in the panel headers generally worsens.

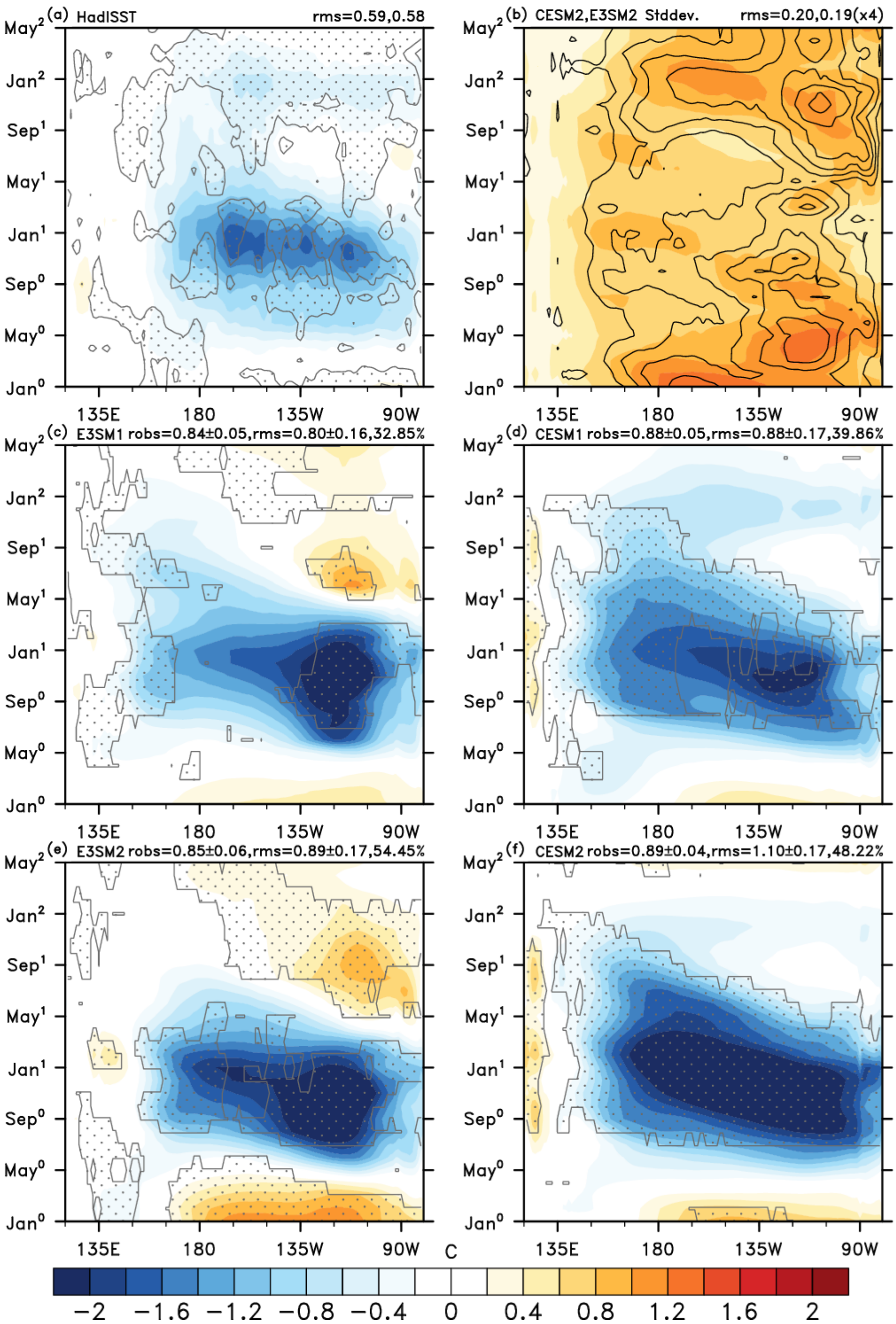

Fig. S3. The observed La Niña hovmoëller pattern in SST (K) estimated from observations (HadISST, **a**) and the standard deviation in the pattern across members of CESM2 (contours) and E3SM2 (lines, **b**). The ensemble-mean patterns estimated from E3SM1 (**c**), CESM1 (**d**), E3SM2 (**e**), and CESM2 (**f**) are also shown. Contours in (**a**) where differences with ERSSTv5 exceed 0.1 K and in (**c-f**) where observations lie outside of each ensemble. Metrics in the panel headers are consistent with those in Fig. 3 in the main text.

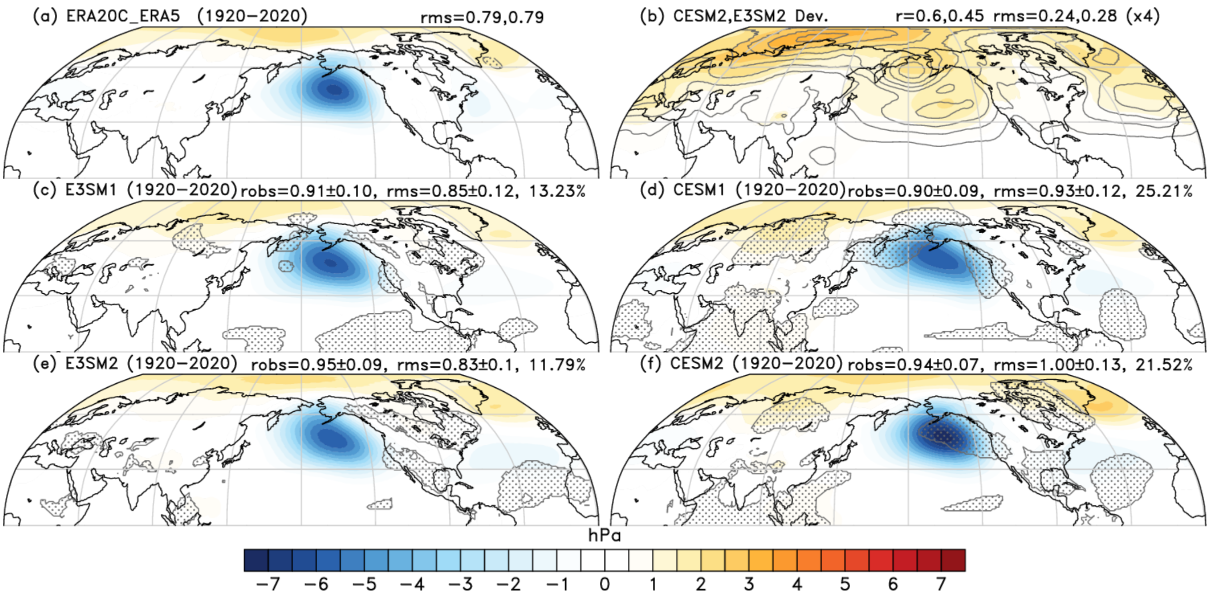

Fig. S4. The observed PNA teleconnection pattern in PSL (hPa) in DJF estimated from observations (ERA20C/ERA5, **a**) and the standard deviation in the pattern across ensemble members from CESM2 (contours) and E3SM2 (lines, **b**). The ensemble-mean patterns estimated from E3SM1 (**c**), CESM1 (**d**), E3SM2 (**e**), and CESM2 (**f**) are also shown. Contours in (**a**) where differences with CERA20C/ERAI exceed 0.3 hPa and in (**c-f**) where observations lie outside of each ensemble. Metrics in the panel headers are consistent with those in Fig. 3 in the main text.

The spatial structure of the PNA teleconnection is shown in Figure S4. The observed pattern (Fig. S4a) is characterized by strong negative values in the North Pacific's Aleutian Low region and weak positive values spanning the Arctic. The pattern of intra-ensemble spread in CESM2 (Fig. S4b) is characterized by the greatest values in the western Arctic and the patterns of spread in CESM2 and E3SM2 agree closely. The ensemble mean pattern in E3SM1 (Fig. S4c) correlates strongly with observations (r=0.91) with a magnitude (rms=0.85) that is stronger than observed (rms=0.80), though the observations fall within the ensemble spread. In CESM1 the strength of the pattern (rms=0.93) is even stronger than in E3SM1, and the pattern correlation is again high (r=0.90). In E3SM2 (r=0.95) and CESM2 (r=0.94), the PNA patterns correlate strongly with observations, though the pattern in CESM2 is stronger than observed (rms=1.00), particularly in the North Pacific Ocean.

High pressure blocking patterns in the mid-latitudes are large-scale modes of extratropical variability most commonly associated with extremes of surface temperature and precipitation (Pfahl, 2014). However, unlike mobile baroclinic weather systems, atmospheric blocking characteristics: onset, duration, and decay, are difficult for models to simulate and predict. This is particularly true during northern winter when events are most prevalent, and the zonal jet interactions are most complex.